Proceedings of Symposium on Ultrasonic Electronics, Vol. 35 (2014) pp. 179-180
3-5 December, 2014

Analysis of spatio-temporal radiated acoustic field from finite aperture transducer - Comparison of FDTD numerical computations and Rayleigh integral method –

有限開口トランスジューサからの時空間放射音場の解析 － FDTD 数値計算とレーリー積分法の比較 －

Akira Yamada[1†], and Yoshio Udagawa[2] ([1]Grad.Bio-Appl.Sys. Eng., Tokyo Univ. of A&T; [2]Imaging Supersonic Laboratories)
山田 晃 [1†], 宇田川義夫 [2] ([1] 東京農工大学 院生物シ応用, [2] アイ・エス・エル)

1. Introduction

Many of the medical equipment and non-destructive inspection devices using ultrasonic waves are adopting the pulse-driven finite aperture piezoelectric vibrator. To build an intended spatio-temporal acoustic field for the design of a device or a vibrator, it is important to analyze the transient radiation acoustic field. It may be considered that most of these have been solved. However, the radiation acoustic field by spatio-temporal discontinuous excitation, as specifically described in this paper, is very different from that by the continuous wave excitation[1],[2]. Its characteristics are not clarified sufficiently. As a theoretical treatment, computation methods based on FDTD (Finite Difference Time Domain) method and Rayleigh integral method are widely used. However, when the fluid medium is excited by the discontinuous source like a rectangular shaped time varying function, computation becomes unstable near the vibrator edges. Validities of the methods are unclear under the critical conditions as the present problem. In this study, the results are compared between the methods while keeping in minds of these points. Based on the obtained results, the behaviors of the spatio-temporal transient acoustic wave field radiated from the finite aperture plate are clarified.

2. Analysis of Transient Radiated Acoustic Field Through FDTD Method

2.1 Analysis Method A finite aperture vibrator with fully backing is placed on the surface of the semi-infinite fluid medium. When the vibrator is excited by the step voltage (Fig1.(a)), the surface displacement of it is a one side trapezoidal function (Fig1.(b)), while the pressure and particle velocity is a unipolar rectangular function (Fig1.(c)). As shown in Fig.2, a circular aperture vibrator is considered with a radius a = 10mm and a center frequency f_0=200 kHz, while the medium is assumed to be water with a longitudinal velocity c = 1497 m/s and a density ρ=1000 kg/m^3. FDTD analysis software (Cyber Logic: WAVE3000) is used to analyze the three-dimensional radiation field of an region with H=80 mm height, W = 50mm width, and D=40mm depth [3]. Considering there is static displacement in this problem, the analysis is conducted while the displacement is selected in the independent variable of the finite difference calculation. The transient radiation acoustic field is analyzed while the driving displacement happens on a one side trapezoidal function with a rise time of T=2.5 μs (This condition is equivalent to a rectangle pressure excitation with a pulse width T=1/2f_0). In order to deal with the discontinuity of the acoustic wave field, the values of grid spacing Δx (=0.1 mm), update increments time Δt (=0.013 μs), and Courant number (=0.2) are much smaller than those in the cases of continuous wave excitation. In addition, the discontinuous parts of the excitation waveform are calculated with roundness as shown in Fig.1(c).

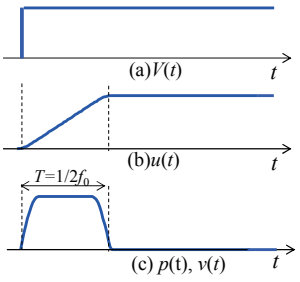

Fig.1 Excitation waveform.

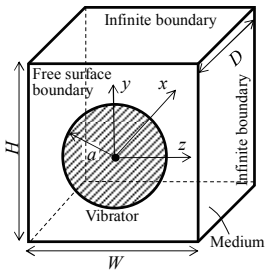

Fig.2 Analysis object.

2.2 Results The calculation result of the radiated acoustic field is shown in Fig.3. As the discontinuity of the acoustic field near the plate edge remains particularly for fluid medium, the numerical computation shows instability. Except for the unstable region near the plate edge, the primary longitudinal plane wave radiated from the transducer surface and the BED (Beam Edge Diffusion) wave with a spherical wavefront radiated from the plate edges can be confirmed. The wave in the central axis immediately after excitation is a unipolar rectangular wave with a plane wavefront (Fig.3(a)). The polarity of BED is negative at the inner side (sunny side) of the transducer and positive at the outside (shadow side) of it. The plane wave and BED wave in the inner side of the transducer get closer with advancing time and finally overlap each other as opposite signs. Therefore, the shape of the pressure distribution also changes from unipolar rectangular wave (Fig3(a)) to bipolar rectangular wave (Fig3(b)), and finally to bipolar

yamada@cc.tuat.ac.jp

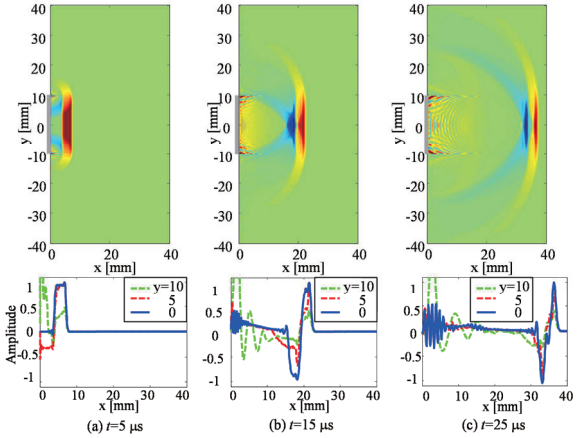

Fig.3 Simulation result of radiated acoustic pressure field using FDTD method.

impulse wave (Fig3(c)) in the distance direction on the central axis. After the front of BED wave and the rear of plane wave cancel each other, the rear part of the former and the front part of the latter will generate a sharp bipolar impulse wave.

3. The Analysis through Rayleigh Integral Method

3.1 Principle A transducer with aperture S is placed on a completely rigid baffle. The time variation of the particle velocity normal direction components on the transducer's surface is denoted by $v_n(t)$. The pressure $p(r_1, t)$ at time t and location r_1 in the right half-plane medium can be expressed by the convolution of the time derivative of $v_n(t)$ and the spatial impulse response h:

$$p(\vec{r}_1,t) = \rho \frac{\partial v_n(t)}{\partial t} * h(\vec{r}_1,t) \quad , \qquad (1)$$

where, ρ is the density, c is the sound speed, and h is the spatial impulse response between the observation point and the transducer aperture surface, which is given by

$$h(\vec{r}_1,t) = \int_S \frac{\delta(t - \frac{|\vec{r}_1 - \vec{r}_2|}{c})}{2\pi |\vec{r}_1 - \vec{r}_2|} dS \quad , \qquad (2)$$

where, r_2 is the coordinates on the transducer surface.

3.2 Method The analysis software FIELD II [4] was used for the calculation. That is, the impulse response of equation (2) was numerically calculated under the same conditions as the previous FDTD analysis. Transducer surface particle velocity $v_n(t)$ was chosen as the rectangular function with width T=2.5μs. By substituting these data into expression (1), the radiation sound pressure at the observation point was calculated.

3.3 Results The calculation results of the radiated acoustic field based using the Rayleigh integral method is shown in Fig.4. The longitudinal plane wave and each acoustic field of BED waves are roughly consistent compared with the results of the FDTD method. However, the result through Rayleigh integral method doesn't show the residual acoustic field generated near the plate edges in the FDTD method. We cannot decide which one has faithfully reflected the experimental

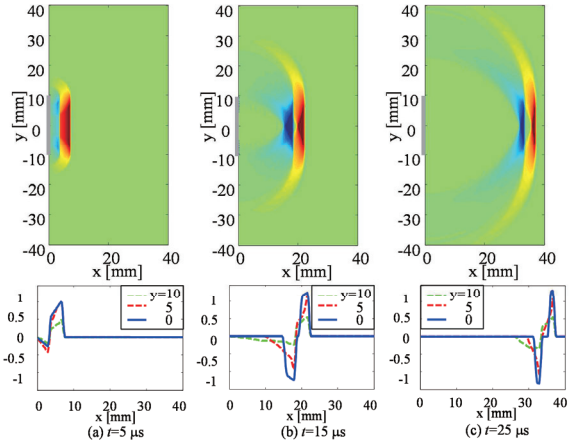

Fig.4 Simulation result of radiated acoustic pressure field using Rayleigh integral method.

results yet. And it will be a challenge to solve from now on.

4. Behavior of Transient Radiated Acoustic Field

4.1 Distance Dependence In the case of continuous wave excitation, the amplitude of the pressure on the central axis of the transducer will decrease in inverse proportion to the distance x, beyond the limit of the near field. In contrary, in the case of rectangular wave excitation, the peak value of the wave stays almost constant and the pulse width is in inverse proportion to the distance. As a result, the high-frequency impulse wave can be propagated anywhere as long as there is no attenuation in the medium.

4.2 Directivity (angular dependence) Fig.5 shows the calculation result of the radiation angular dependency of BED wave's sound pressure on the outer side of the transducer. Although FDTD and Rayleigh integral methods show large difference on short ranged results, they do have the similar characteristics on the long distance. Note that there isn't any side lobe dip as in the case of continuous wave acoustic excitation, either.

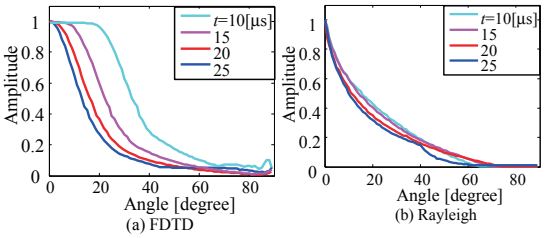

Fig.5 Angular dependence of the outer BED wave amplitude.

References

1. Y.Udagawa, *Introduction to Ultrasonic Wave Technique – Transducer, Pulser, Receiver and Device-*, Nikkan Kogyo Shimbun, Tokyo (2010).
2. A.Yamada and Y.Udagawa, The 34th Symp. Ultrason. Elect. **34** (2013) pp.11-12(1J2-6).
3. R.S.Schechter, H.H.Chaskelis, R.B.Mignogna, P.P.Delsanto, Science, **265** (Aug.1994) pp.1188-92.
4. J. A. Jensen and N. B. Svendsen. IEEE Trans. Ultrason., Ferroelec., Freq. Contr., 39, (1992) pp.262–267.